Journal of Physiology (1990), **431**, *pp.* 243–267
With 13 figures
Printed in Great Britain

MEMBRANE DEPOLARIZATION AND INTRACELLULAR Ca^{2+} INCREASE CAUSED BY HIGH EXTERNAL Ca^{2+} IN A RAT CALCITONIN-SECRETING CELL LINE

BY NAOHIDE YAMASHITA* AND THE LATE SUSUMU HAGIWARA

From the Department of Physiology, Jerry Lewis Neuromuscular Research Center and the Ahmanson Laboratory of Neurobiology in the Brain Research Institute, University of California School of Medicine, Los Angeles, CA 90024, USA

(*Received 9 March 1990*)

SUMMARY

1. Calcitonin secretion is regulated by the external Ca^{2+} concentration ($[Ca^{2+}]_o$) via a rise in intracellular Ca^{2+} concentration ($[Ca^{2+}]_i$). The mechanism which couples an increase in $[Ca^{2+}]_o$ to an increase in $[Ca^{2+}]_i$ was explored in a rat calcitonin-secreting cell line (rMTC 44-2). $[Ca^{2+}]_i$ was monitored using Fura-2 AM, and the membrane potential or current was simultaneously measured.

2. Using the conventional whole-cell clamp, tetrodotoxin-sensitive voltage-gated Na^+ channels, T- and L-type Ca^{2+} channels, and three types of K^+ channels, the delayed K^+ channel, the A-channel and the inward-rectifying channel were observed.

3. Using the nystatin-perforated whole-cell-clamp technique, the resting potential measured under current clamp in standard extracellular medium was $-59{\cdot}0 \pm 5{\cdot}0$ mV (mean $\pm$ S.D., $n = 25$), and the input resistance was $3{\cdot}9 \pm 1{\cdot}9$ GΩ ($n = 10$). In 0·5 mM $[Ca^{2+}]_o$ most cells (22/25) showed spontaneous action potentials.

4. An increase in $[Ca^{2+}]_o$ depolarized the cell membrane and elevated $[Ca^{2+}]_i$ even in the presence of 10 μM-tetrodotoxin. The rise in $[Ca^{2+}]_i$ was greatly reduced when action potentials were inhibited by applying hyperpolarizing current. The increase in $[Ca^{2+}]_i$ saturated with 3–4 mM $[Ca^{2+}]_o$. In 3 mM $[Ca^{2+}]_o$, $[Ca^{2+}]_i$ was $188{\cdot}9 \pm 40{\cdot}5\%$ ($n = 12$) of that in 0·5 mM $[Ca^{2+}]_o$.

5. In high $[Ca^{2+}]_o$ the duration of action potentials was prolonged, but the action potential frequency did not always increase. In some cases it even decreased in high $[Ca^{2+}]_o$.

6. Two types of action potential were observed in high $[Ca^{2+}]_o$, one with a shorter duration and the other with a longer duration. $[Ca^{2+}]_i$ transiently increased in association with the long-duration action potentials. These long-duration action potentials were also accompanied by a larger after-hyperpolarization.

7. Under voltage clamp, high $[Ca^{2+}]_o$ caused a membrane conductance increase to Na^+ ions.

8. Even when the membrane potential was clamped at a level below the threshold for Ca^{2+} channel activation, high $[Ca^{2+}]_o$ provoked an increase of $[Ca^{2+}]_i$ which was

* Present address to which reprint requests should be sent: Fourth Department of Internal Medicine, Tokyo University Branch Hospital, 3-28-6 Mejirodai, Bunkyo-ku, Tokyo 112, Japan.

MS 8338

composed of an initial transient increase followed by a sustained increase, indicating an involvement of mechanisms other than Ca^{2+} influx through voltage-gated channels. The sustained increase was more frequently observed than the initial transient increase. The amplitude of the sustained phase was dependent on $[Ca^{2+}]_o$, and in 5 mM $[Ca^{2+}]_o$ it was $120{\cdot}9 \pm 18{\cdot}9\%$ (103–194%) ($n = 58$) of that in 0·5 mM $[Ca^{2+}]_o$.

9. Under voltage clamp, a brief application (500 ms) of high $[Ca^{2+}]_o$ caused an initial transient increase which reached the maximum 10–15 s after high $[Ca^{2+}]_o$ application, indicating that Ca^{2+} ions mobilized from the internal store are involved in the initial transient increase.

10. Sr^{2+} substituted for Ca^{2+} in increasing the membrane conductance and $[Ca^{2+}]_i$ under voltage clamp, whereas Mg^{2+} and Co^{2+} did not. Nitrendipine (1 μM) and Bay K 8644 (1 μM) had little effect on membrane conductance and on $[Ca^{2+}]_i$ under voltage clamp.

11. In rat GH_3 cells, high $[Ca^{2+}]_o$ neither depolarized the cell membrane nor changed $[Ca^{2+}]_i$.

12. Three modes of $[Ca^{2+}]_i$ increase are discussed. One mode is an influx through voltage-gated Ca^{2+} channels. The second one, which manifested as the initial transient increase of $[Ca^{2+}]_i$ under voltage clamp, may be ascribed to a mobilization from the internal Ca^{2+} store. The third one, which constituted the sustained increase, is undetermined.

INTRODUCTION

Secretion of peptide hormones is regulated by various agonists and antagonists via their specific cell membrane receptors. The regulation of calcitonin secretion is unique because the extracellular Ca^{2+} concentration ($[Ca^{2+}]_o$) within a physiological range is the major agonist. It has been reported that in the rat medullary thyroid carcinoma C-cell line, rMTC cells, secretion of calcitonin and neurotensin is enhanced by increasing $[Ca^{2+}]_o$ (Gagel, Zeytinoglu, Voelkel & Tashjian, 1980; Zeytinoglu, Gagel, Tashjian, Hammer & Leeman, 1983), and that the intracellular Ca^{2+} concentration ($[Ca^{2+}]_i$) measured by Quin-2 increases in response to a rise in $[Ca^{2+}]_o$ (Hishikawa, Fukase, Takenaka & Fujita, 1985; Fried & Tashjian, 1986; Haller-Brem, Muff, Petermann, Born, Roos & Fischer, 1987). Parathyroid hormone and renin secretion are also regulated by $[Ca^{2+}]_o$ although the secretion of parathyroid hormone and renin is inhibited by high $[Ca^{2+}]_o$. In parathyroid cells (Nemeth & Scarpa, 1987; Schoback, Mambreno & Mcghee, 1988) and in juxtaglomerular cells (Kurtz & Penner, 1989) it has been reported that high $[Ca^{2+}]_o$ increases $[Ca^{2+}]_i$ in the absence of other stimuli, similar to rMTC cells.

rMTC cells exhibit action potentials which depend on Na^+ and Ca^{2+} ions (Sand, Ozawa & Gautvik, 1981). Ca^{2+} influx through voltage-gated channels during action potentials has been implicated in hormone release in various excitable endocrine cells (Ozawa & Sand, 1986). In calcitonin-secreting cells, voltage-gated Ca^{2+} channels have been implicated in hormone secretion because increasing external K^+ concentration, or applying Ca^{2+} channel agonists, stimulates hormone secretion (Gagel *et al.* 1980; Hishikawa *et al.* 1985; Cooper, Borosky, Farrell & Steinsland, 1986; Muff, Nemeth, Haller-Brem & Fisher, 1988). However, it has not been clarified

how $[Ca^{2+}]_i$ increases in high $[Ca^{2+}]_o$ and direct evidence for the involvement of voltage-gated Ca^{2+} channels in increasing $[Ca^{2+}]_i$ is still lacking. Ozawa & Sand (1986) have pointed out that the inward driving force for Ca^{2+} is only slightly affected by the modest change of $[Ca^{2+}]_o$ within the physiological range, and that it seems difficult to ascribe the increase of $[Ca^{2+}]_i$ in high $[Ca^{2+}]_o$ simply to enhanced driving force for Ca^{2+}. In parathyroid cells alteration of $[Ca^{2+}]_o$ causes membrane potential changes (Bruce & Anderson, 1979; Sand, Ozawa & Hove, 1981; Lopez-Barneo & Armstrong, 1983; Morrissey & Klahr, 1983). It is possible, therefore, that in calcitonin-secreting cells the Ca^{2+} action potential activity may be modulated by high $[Ca^{2+}]_o$ through a membrane electrical phenomena.

In the conventional whole-cell-clamp configuration the leakage current progressively increased during recordings and the wash-out of various internal molecules essential for hormone secretion may be a serious problem. In this paper, therefore, we applied the perforated whole-cell-clamp technique (Horn & Marty, 1988) to rMTC 44-2 cells for recording the membrane potential or current, in conjunction with the measurement of $[Ca^{2+}]_i$ using Fura-2 AM. A preliminary report of this work has already been published as an abstract (Yamashita & Hagiwara, 1990).

METHODS

Cell culture. rMTC 44-2 cells were kindly provided by Dr A. H. Tashjian Jr (Harvard Medical School, USA). Cells were cultured in Dulbecco's modified Eagle's medium supplemented with 15% horse serum and subcultured every 12–14 days. At the time of subculturing some cells were plated on polylysine-coated glass cover-slips and used for experiments after 4–7 days. The diameter of the cell was 10–15 μm.

Electrophysiological studies. The whole-cell variation of the patch electrode voltage-clamp technique (Hamill, Marty, Neher, Sakmann & Sigworth, 1981) and the perforated whole-cell-clamp technique (Horn & Marty, 1988) were used. The former method was used for analysing voltage-gated channel currents and the latter for recording the changes of the membrane potential and current in response to an increase of $[Ca^{2+}]_o$. The standard patch electrode solution contained (in mM): 95 potassium aspartate, 47·5 KCl, 1 $MgCl_2$, 0·1 EGTA (tetramethylammonium (TMA) salt), 10 HEPES (TMA salt, pH 7·2). This solution was mainly used for the perforated whole-cell clamp. For blocking the outward current, K^+ ions were replaced with Cs^+ ions. In the case of the whole-cell clamp the EGTA concentration in the patch electrode solution was increased to more than 5 mM by isosmotically replacing aspartate because the leakage current increased soon after formation of the whole-cell configuration with the low EGTA internal solution. Changes in the composition of the internal solution are noted in Results or figure legends. The standard extracellular medium was composed of (in mM): 128 NaCl, 5 KCl, 1 $MgCl_2$, 0·5 $CaCl_2$, 10 HEPES (Na salt, pH 7·4). In high-Ca^{2+} media, Ca^{2+} concentration was increased by isosmotic replacement of Na^+ ions. The media containing high concentrations of divalent cations other than Ca^{2+}, such as 5 mM-Sr^{2+} or 5 mM-Mg^{2+}, were made in a similar manner. In high-K^+ medium the concentration of K^+ ions was increased by isosmotic replacement of Na^+ ions. In Na^+-free medium all Na^+ ions were replaced with TMA ions. The extracellular medium was continuously perfused during recording using a peristaltic pump and high $[Ca^{2+}]_o$ was applied by changing the perfused medium. In some cases high $[Ca^{2+}]_o$ was administered through a glass capillary with a tip diameter of about 5 μm by applying positive pressure for 500 ms (puff method). The liquid junction potential between the standard extracellular solution and other solutions used (internal and external) was directly measured using a 3 M-KCl electrode as a reference. The value of liquid junctional potential (-8 to 2 mV) was corrected in each experiment. A List EPC-7 amplifier was used for recording the membrane current and potential. Application of voltage or current pulses, data acquisition, and analysis were done with an AST premium/286 computer using the Axolab 1100 interface and pCLAMP program (Axon Instruments, CA). All experiments were performed at room temperature (22–25 °C).

Glass capillaries of 1·5 mm diameter with a filament (World Precision Instruments, Inc. CT, USA) were used to fabricate electrodes for both the whole-cell clamp and the perforated whole-cell clamp. They were thickly coated with Sylgard and fire-polished before use. The patch electrode resistance used in these studies was in the range of 5–8 MΩ. Methods for the conventional whole-cell clamp were essentially the same as described by Hamill *et al.* (1981). The amplitude of membrane current recorded under conventional whole-cell clamp was less than 350 pA and series resistance compensation (70–90 %) was used, so that the error of the clamped potential was small and was ignored during analyses. The records obtained using the conventional whole-cell-clamp technique were corrected for the leakage current using the slope of the current from −90 to −60 mV.

Perforated whole-cell clamp. Nystatin was purchased from Sigma (St Louis, MO, USA) and a fresh stock solution was made in dimethylsulphoxide (50 mg/ml) daily. Shortly before recording, the stock solution was diluted with the patch electrode solution (final nystatin concentration, 200 μg/ml). This solution was kept for 1–2 h. Because it was difficult to form a gigaseal if the nystatin solution was filled to the tip of the electrode, the following procedure was taken. First the tip of an electrode was dipped in the internal solution without nystatin for 10–20 s. Then, keeping the tip of the electrode in the solution, the pipette was backfilled with the nystatin-containing internal solution. Immediately after filling, the electrode was mounted on the manipulator and was brought in contact with the cell surface as soon as possible. Then negative pressure of less than 5 cmH_2O was applied to the inside of the electrode. Within 1–2 min the seal resistance increased to as much as several tens of gigaohms. After formation of a gigaseal the negative pressure was released. The capacitance of the electrode was compensated after formation of the gigaseal. The series resistance was calculated under voltage clamp by dividing the applied hyperpolarizing voltage (10 mV) from the holding potential (−55 to −58 mV) by the amplitude of the initial capacitive surge. Within a few minutes after formation of the gigaseal the series resistance began to decrease, and fell below 100 MΩ after 5–15 min. Current-clamp recordings were then started. Voltage-clamp recordings were made after the series resistance fell below 50 MΩ. Series resistance compensation was not used in the case of perforated whole-cell clamp because the series resistance was checked during recording with the above method and because the series resistance changed during recording. Unless otherwise noted, the amplitude of the membrane current recorded with the perforated whole-cell clamp did not exceed 50 pA, which did not cause a serious error in the clamped potential. However, in some cases in which greater amplitudes of membrane current were recorded, such as shown Fig. 8, the membrane potential was corrected by the formula, $V_c = V - R_s \times I$, where V_c is the corrected membrane potential, V, clamped potential, R_s, series resistance, and I, membrane current.

Measurement of $[Ca^{2+}]_i$. Cells were loaded with Fura-2 by incubating with 2 μM-Fura-2 AM in Hanks' balanced salt solution containing 0·1 % bovine serum albumin for about 1 h at room temperature. Then the cells were washed three times with standard extracellular medium. Fura-2 was excited alternately by light at 340 and 380 nm using a rotating filter wheel (frequency, 20–30 Hz). Fluorescent light was collected from a pin-hole area of 15 μm diameter in the centre of the field of view where a single cell was placed. The fluorescence intensity was measured through a 500 nm filter with a photomultiplier. The signal at 340 nm was divided by that at 380 nm and the ratio was used for determining $[Ca^{2+}]_i$. $[Ca^{2+}]_i$ shown in the figures was filtered with a bandwidth of 1 Hz (rise time from 10 to 90 % = 300 ms) in order to reduce the noise. The data were not corrected for autofluorescence which was less than 5 % of the Fura-2 signal. The value of 340/380 signal ratio varied considerably among experiments and it has been known that it is difficult to determine the absolute value of $[Ca^{2+}]_i$ using Fura-2 AM (Jacob, Murphy & Lieberman, 1987; Lewis, Goodman, John & Barker, 1988). Therefore relative changes in $[Ca^{2+}]_i$ are expressed as percentage of the basal level which was $[Ca^{2+}]_i$ level in 0·5 mM-Ca^{2+} medium in each cell. This value does not mean the change in the absolute value of $[Ca^{2+}]_i$ because the ratio of Fura-2 signals was not proportional to $[Ca^{2+}]_i$. The time-dependent loss of Fura-2 signal of the cells under perforated whole-cell clamp was not greater than that of the control. It appears, therefore, that the Fura-2 molecule did not diffuse into the recording electrode through pores formed by nystatin.

RESULTS

Voltage-gated channel currents in rMTC 44-2 cells

In order to interpret results with the perforated whole-cell-clamp technique we first examined voltage-gated channel currents with the conventional whole-cell-

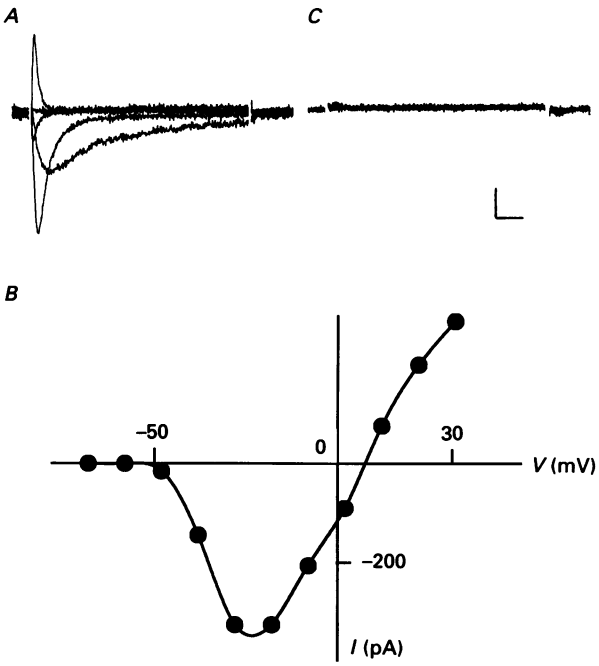

Fig. 1. Na^+ channel current. *A*, Na^+ current recorded in the 1/10 Na^+ (13·3 mM), 1 mM-Co^{2+} medium containing no Ca^{2+}. The patch electrode solution contained 10 mM-Na^+, 102·5 mM-Cs^+ and 20 mM-EGTA. The holding potential was −68 mV. Current records at the depolarizing potentials to −58, −38, −18, 2 and 22 mV are shown. Leakage current was subtracted. *B*, *I–V* relation of the record in *A*. *C*, membrane current recorded in the medium containing 5 μM-TTX. Holding and test potentials were the same as those in *A*. Current amplitude (vertical) and time scale (horizontal) bar are equal to 100 pA and 5 ms, respectively.

clamp method. Na^+ and Ca^{2+} components in the action potential have previously been reported in rMTC cells with the glass microelectrode technique (Sand *et al.* 1981).

Na^+ current

The isolation of Na^+ current was achieved by blocking Ca^{2+} current with external Co^{2+} ions and by eliminating outward K^+ currents with internal Cs^+ ions in the standard medium. The peak amplitude of the maximum Na^+ current was more than 1 nA and gave rise to a serious error of the clamped potential. To avoid this problem

recording of Na^+ current was performed in 1/10 Na^+ (13·3 mM) medium. Figure 1*A* shows the Na^+ current recorded in 1/10 Na^+, 1 mM-Co^+ medium. The patch electrode solution contained 10 mM-Na^+, 102·5 mM-Cs^+ and 20 mM-EGTA. The holding potential was −68 mV. When the membrane was depolarized, the inward current

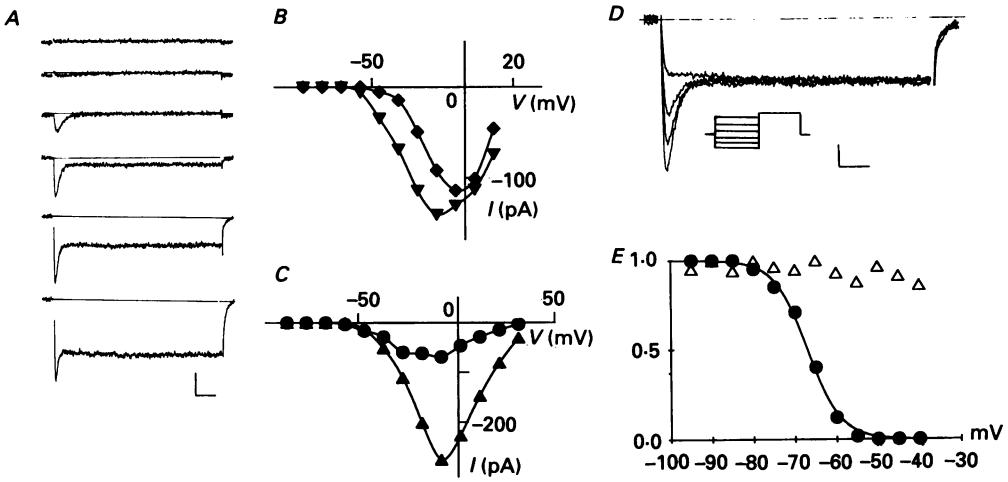

Fig. 2. Ca^{2+} channel current. *A*, Ba^{2+} current through Ca^{2+} channels recorded in 3 mM-Ba^{2+} medium containing 5 μM-TTX. The patch electrode solution contained 112·5 mM-Cs^+ and 20 mM-EGTA. The holding potential was −85 mV. Current records at −75, −65, −55, −45, −35 and −25 mV are shown. Current amplitude and time scale bar are equal to 40 pA and 100 ms, respectively. The continuous line in the record indicates the zero current level. Leakage current was subtracted. *B*, *I–V* relations of Ba^{2+} current shown in *A*. ▼, the peak amplitude of the Ba^{2+} current; ◆, the amplitude of the Ba^{2+} current at the end of the pulse. *C*, comparison of *I–V* relations at the peak of the Ba^{2+} current obtained from a cell in 1 mM (●) and 5 mM (▲) Ba^{2+} media containing 5 μM-TTX. The holding potential was −85 mV. The composition of the internal solution was the same as in *A*. *D*, changes of Ba^{2+} current by application of 200 ms pre-pulse from the holding potential of −85 mV to the fixed potential of −35 mV. The inset indicates the protocol. The pre-pulse potentials were −95, −70, −65 and −55 mV. The composition of the internal solution was the same as in Fig. 2*A*. Current amplitude and time scale bar are equal to 20 pA and 50 ms, respectively. The continuous line in the figure indicates the zero current level. Leakage current was subtracted. *E*, steady-state inactivation curve of T (●) and L (△) types of Ca^{2+} channels obtained from the record in *D*. Current amplitude was normalized by dividing by the maximum current. Continuous line was drawn according to the formula, $h = 1/[1+\exp\{(V-V_{\frac{1}{2}})/K_h\}]$, where V is the pre-pulse potential and $V_{\frac{1}{2}}$ is the potential at which the inactivation parameter h becomes 0·5 (−67 mV). The slope parameter K_h was set to 4·0.

first appeared at a potential step to −48 mV. The peak amplitude of the inward current increased with greater depolarizing potential steps, and both the activation and inactivation processes became faster. The current–voltage (*I–V*) relation of the membrane current is shown in Fig. 1*B*. The reversal potential was 7·0 mV, which is near the equilibrium potential of Na^+ ions (7·2 mV). The inward current was completely inhibited either by removing extracellular Na^+ ions or by adding 5 μM-

tetrodotoxin (TTX) to the Na^+-containing medium (Fig. 1*C*). These properties are characteristic of the voltage-gated Na^+ channel.

Ca^{2+} currents

To isolate Ca^{2+} currents the Na^+ current was blocked with 5 μM-TTX and outward K^+ currents were again eliminated with internal Cs^+. Figure 2*A* shows the Ca^{2+}

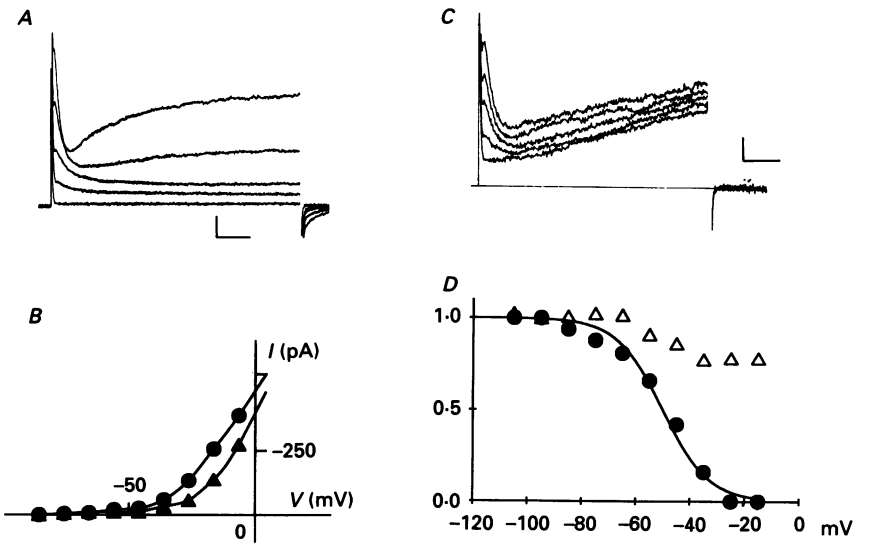

Fig. 3. Outward K^+ currents. *A*, outward current recorded in Na^+-free, 1 mM-Co^{2+} medium. The patch electrode solution contained 112·5 mM-K^+ and 20 mM-EGTA. The holding potential was −85 mV. Current records were obtained at the test potentials of −75, −35, −25, −15 and −5 mV. Current amplitude and time scale bar are equal to 50 pA and 20 ms, respectively. *B*, *I–V* relations of the membrane currents in *A*. ●, the peak amplitude of the fast-inactivating current; ▲, the amplitude of the outward current at the end of the depolarizing pulse. *C*, changes of the outward current with 100 ms pre-pulse from the holding potential of −55 mV to the fixed potential of −5 mV. Pre-pulse potentials were −105, −55, −45, −35 and −25 mV. Current amplitude and time scale bar are equal to 30 pA and 10 ms, respectively. *D*, steady-state inactivation of outward current. ●, the amplitude of fast-inactivating outward current (A-current); △, the amplitude of the outward current at the end of the depolarizing pulse (delayed K^+ current). The continuous line in the figure was drawn according to the same formula as used in Fig. 3*B*. $V_{\frac{1}{2}}$ was −50 mV and K_h was set to 8·5.

channel current obtained in 3 mM-Ba^{2+} medium. The pipette contained 112·5 mM-Cs^+ and 20 mM-EGTA. The holding potential was −85 mV. Clearly there were a fast-inactivating inward current and a steady inward current, the latter being prominent at potentials less negative than −45 mV. The *I–V* relations at the peak of inward current (▼) and at the end of the voltage steps (◆) are shown in Fig. 2*B*. Figure 2*C* compares *I–V* relations at the peak of Ba^{2+} current recorded in 1 mM-Ba^{2+} (●) and 5 mM-Ba^{2+} (▲) media both containing 5 μM-TTX. The peak of the maximum inward current in 5 mM-Ba^{2+} medium was about by 3 times that in 1 mM-Ba^{2+} medium.

Figure 2*D* shows representative records of the Ba^{2+} current obtained in 3 mM-Ba^{2+} medium when a 200 ms pre-pulse of various amplitudes was applied from the holding potential of −85 mV (see protocol in the inset). The fixed potential level of the test pulse was −35 mV. The peak amplitude of the fast-inactivating current was determined by subtracting the steady inward current evoked following a −50 mV pre-pulse from the current evoked following the pre-pulses of various amplitudes. The normalized residual current was plotted against the pre-pulse potential and is shown in Fig. 2*E* (●), as is the amplitude of the normalized steady current measured at the end of the test pulse (△). The peak amplitude of fast-inactivating current was reduced as pre-pulse amplitude increased, whereas the steady current was not. From these findings it was concluded that the fast-inactivating Ba^{2+} current was carried by a transient (T)-type Ca^{2+} channel and the steady Ba^{2+} current was via a long-lasting (L)-type Ca^{2+} channel. The threshold for the steady inward current was about 20 mV more positive than that of the fast-inactivating current (Fig. 2*A*). Both inward currents were completely inhibited when 5 mM-Co^{2+} was added to the external medium (data now shown). In Ca^{2+}-containing medium similar T- and L-type Ca^{2+} currents were observed.

Outward K^+ currents

Figure 3*A* shows the outward currents recorded in a Na^+-free solution with 1 mM-Co^{2+}. The holding potential was −85 mV. The patch electrode contained 112·5 mM-K^+ and 20 mM-EGTA. The outward current consisted of a fast-inactivating component and a steady component. The *I–V* relations at the peak of the fast-inactivating current (●) and at the end of the depolarizing pulse (▲) are shown in Fig. 3*B*. Figure 3*C* shows the changes of the outward current when 100 ms pre-pulses were applied from a holding potential of −55 mV. The test pulse was to −5 mV. The amplitude of the fast-inactivating current was determined by subtracting the test outward current evoked following the pre-pulse to −15 mV from the current evoked following the pre-pulses of various amplitudes. The residual current is plotted against pre-pulse potential in Fig. 3*D* (●), where the amplitude of the outward current at the end of pulse is also plotted (△). The fast-inactivating outward current was progressively inhibited by increasing the pre-pulse amplitude, whereas the steady outward current was much less affected. Both outward currents were suppressed when the internal solution contained Cs^+ instead of K^+. These results suggest that the fast-inactivating outward current is an A-type K^+ current (Hagiwara, 1983), while the steady outward current is a delayed-type K^+ current.

Inward-rectifying K^+ current

Figure 4*A* shows the inward-rectifying current obtained in the standard and in 20 mM-K^+ media. Membrane currents were recorded by hyperpolarizing the membrane potential from the holding potential of −45 mV. The patch electrode contained standard internal solution. *I–V* relations of the inward-rectifying current are shown in Fig. 4*B*. In 20 mM-K^+ medium the membrane current amplitude increased and the threshold potential for inward current was shifted to a more positive voltage, indicating that the inward-rectifying current is carried by K^+ ions in a similar manner to the anomalous rectifying current reported in other cells

(Hagiwara, 1983). In addition to these voltage-gated K^+ channel currents, rMTC 44-2 cells manifest the Ca^{2+}-activated K^+ current as described later.

Effect of high $[Ca^{2+}]_o$

Membrane depolarization and a rise in $[Ca^{2+}]_i$ *caused by high* $[Ca^{2+}]_o$

In the conventional whole-cell-clamp method the leakage current progressively increased following establishment of the whole-cell clamp probably as a result of

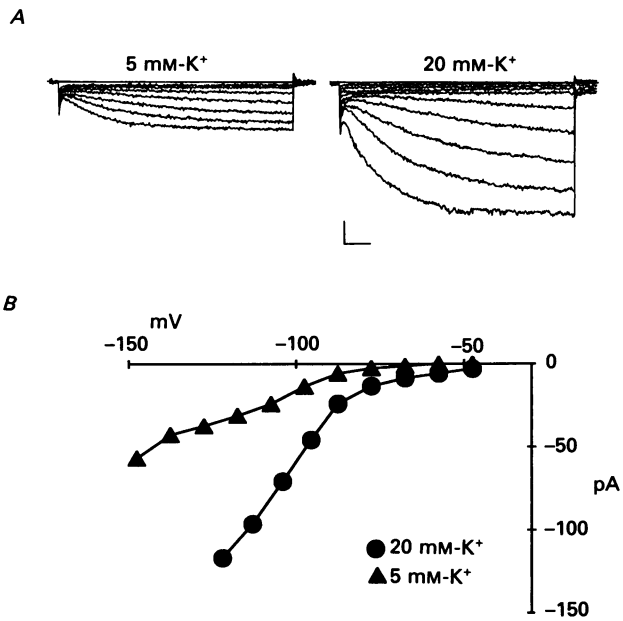

Fig. 4. Inward-rectifying current. *A*, membrane currents recorded in the standard (5 mM-K^+) and 20 mM-K^+ medium. The holding potential was −37 mV. Membrane currents at every 10 mV step from −147 to −87 mV are shown in 5 mM-K^+ medium and those from −127 to −57 mV are shown in 20 mM-K^+ medium. These records were obtained with the perforated whole-cell-clamp technique. The patch electrode contained the standard internal solution. Current amplitude and time scale bar are equal to 20 pA and 200 ms, respectively. *B*, *I–V* relation of membrane currents shown in *A*. The series resistance was 30 MΩ and the clamped potential in 20 mM-K^+ medium was corrected by the formula described in Methods.

dialysis of intracellular substrates. To avoid such problems the following data were obtained using the perforated whole-cell-clamp technique.

With this method the resting potential recorded under current-clamp was $-59{\cdot}0 \pm 5{\cdot}0$ mV (mean ± S.D., $n = 25$) in standard medium. The input resistance measured by applying a hyperpolarizing current pulse (5–10 pA) was $3{\cdot}9 \pm 1{\cdot}9$ GΩ ($n = 10$). Figure 5 shows two representative records of the membrane potential response to a rise in $[Ca^{2+}]_o$ (upper panels) and also shows $[Ca^{2+}]_i$ which was measured simultaneously (lower panels). In Fig. 5*A* the resting potential was about −59 mV

in 0·5 mM-Ca^{2+} medium and spontaneous action potentials were observed. The majority of cells (22/25) showed spontaneous action potentials in 0·5 mM-Ca^{2+} medium. The application of 3 mM-Ca^{2+} depolarized the cell by about 10 mV and caused a significant rise in $[Ca^{2+}]_i$. When the external medium was changed from

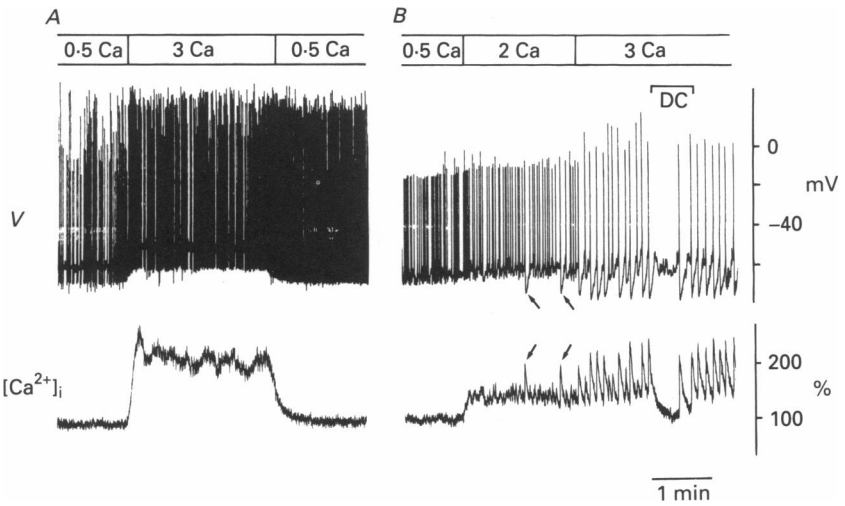

Fig. 5. Membrane depolarization and a concurrent rise of $[Ca^{2+}]_i$ in high $[Ca^{2+}]_o$. Upper panels indicate the membrane potential and lower panels indicate $[Ca^{2+}]_i$. One hundred per cent $[Ca^{2+}]_i$ means the basal level of $[Ca^{2+}]_i$ in 0·5 mM-Ca^{2+} medium. The membrane potential changes were recorded under current clamp with the perforated whole-cell-clamp technique. The concentration of external Ca^{2+} is shown in the figure. The patch electrode contained the standard internal solution. Arrows in *B* show action potentials with a prolonged after-hyperpolarization in 2 mM-Ca^{2+} medium which was associated with a transient rise in $[Ca^{2+}]_i$. DC in *B* indicates the period during which hyperpolarizing current (4 pA) was applied and action potentials were inhibited.

3 mM $[Ca^{2+}]_o$ to 0·5 mM $[Ca^{2+}]_o$, the membrane potential returned close to the original level, as did $[Ca^{2+}]_i$. Although in this record action potential frequency rose when $[Ca^{2+}]_o$ was increased, it was generally observed that the frequency of action potentials was not correlated to $[Ca^{2+}]_o$, both increases and decreases of action potential frequency occurring in response to elevation of $[Ca^{2+}]_o$. In the experiment shown in Fig. 5*B* increasing $[Ca^{2+}]_o$ from 0·5 to 2 mM depolarized the membrane and increased $[Ca^{2+}]_i$ although the membrane depolarization was smaller than that shown in Fig. 5*A*. Two after-hyperpolarizations were observed accompanied by a sharp rise in $[Ca^{2+}]_i$ (see arrows). Upon elevation of $[Ca^{2+}]_o$ to 3 mM most action potentials were followed by large after-hyperpolarizations each accompanied by a sharp rise in $[Ca^{2+}]_i$. In this condition, application of a small hyperpolarizing current inhibited spontaneous action potentials and greatly reduced the $[Ca^{2+}]_i$ increase (see the period marked by DC in the figure). This indicates that Ca^{2+} influx through voltage-gated Ca^{2+} channels during action potentials is important for increasing $[Ca^{2+}]_i$ in high $[Ca^{2+}]_o$ even though the frequency of action potentials does not correlate with $[Ca^{2+}]_o$.

Figure 6*A* compares the characteristics of the individual action potential (upper panel) and the changes in $[Ca^{2+}]_i$ (lower panel) in 0·5 and 2 mM-Ca^{2+} media taken from the record of Fig. 5*B* on an expanded time scale. There were two types of action potential in 2 mM-Ca^{2+} medium, that is, one with a shorter duration (middle) and the

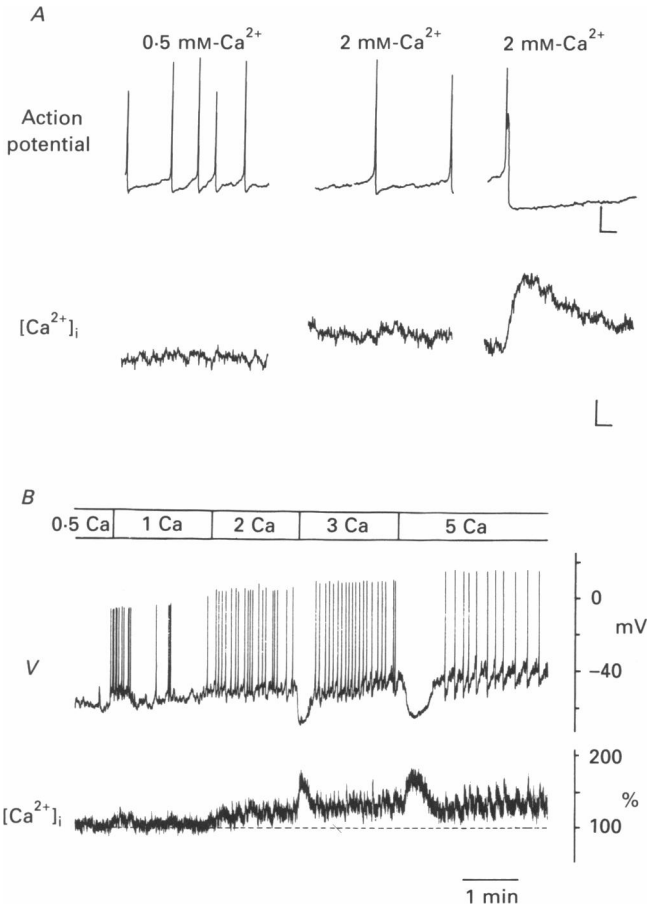

Fig. 6. *A*, comparison of action potential and $[Ca^{2+}]_i$ between 0·5 mM-Ca^{2+} and 2 mM-Ca^{2+} media. Action potentials (upper panel) and $[Ca^{2+}]_i$ (lower panel) were taken from the record of Fig. 5*B*. The potential and time scale bar in the upper panel are equal to 20 mV and 400 ms, respectively and the vertical scale bar in the lower panel indicates the change of $[Ca^{2+}]_i$ equal to 20 % of the basal level. Time scale in the lower panel is the same as that in the upper panel. *B*, changes of membrane potential and $[Ca^{2+}]_i$ in various concentrations of $[Ca^{2+}]_o$ recorded under current clamp with the perforated whole-cell-clamp technique. The patch electrode contained the standard internal solution. The upper panel indicates the membrane potential and lower panel, $[Ca^{2+}]_i$. The dashed line in the lower panel indicates the basal level of $[Ca^{2+}]_i$.

other with a longer duration (right). Only the latter was followed by a prominent after-hyperpolarization. Although not clear in Fig. 6*A*, the duration of the action potential in 2 mM-Ca^{2+} shown in the middle panel was prolonged as compared with that in 0·5 mM-Ca^{2+} (left). In 2 mM-Ca^{2+} medium a transient rise in $[Ca^{2+}]_i$ occurred

with the longer duration action potential, and the rise in $[Ca^{2+}]_i$ was longer lasting than the action potential. In contrast, the shorter duration action potential in 0·5 or 2 mM Ca^{2+} was not associated with a transient rise in $[Ca^{2+}]_i$.

Dependence of $[Ca^{2+}]_i$ on $[Ca^{2+}]_o$ under current clamp

Figure 6*B* illustrates the dependence of the membrane potential and $[Ca^{2+}]_i$ on $[Ca^{2+}]_o$. The dashed line in the lower panel indicates the level of $[Ca^{2+}]_i$ in 0·5 mM-Ca^{2+} medium (basal level). This cell did not generate spontaneous action potentials in 0·5 mM-Ca^{2+} medium. In 1 mM-Ca^{2+} the membrane depolarized and a short burst of action potentials was observed. The increase in $[Ca^{2+}]_i$ was limited to a small rise which occurred during the short burst of action potentials. In 2 mM-Ca^{2+} the membrane further depolarized accompanied by an increase in action potential frequency and $[Ca^{2+}]_i$ increased to 120% of the basal level. Increasing $[Ca^{2+}]_o$ from 2 to 3 mM hyperpolarized the membrane for about 15 s. Concomitant with the membrane hyperpolarization, $[Ca^{2+}]_i$ temporarily increased to 180% of the basal level and thereafter fell to a new steady level (140% of basal). Both the initial membrane hyperpolarization and the transient increase in $[Ca^{2+}]_i$ were also observed upon raising $[Ca^{2+}]_o$ to 5 mM but the duration (40 s) was longer. The action potential duration was also prolonged in 5 mM-Ca^{2+} medium. The initial membrane hyperpolarization induced by high $[Ca^{2+}]_o$ was observed in three of twenty-five cells examined.

Figure 7*A* shows the relationship between the increase of $[Ca^{2+}]_i$ and $[Ca^{2+}]_o$ obtained in five representative cells. The increase of $[Ca^{2+}]_i$ at a given $[Ca^{2+}]_o$ was calculated by dividing the integrated area of $[Ca^{2+}]_i$ by the period during which high $[Ca^{2+}]_o$ was applied. The basal $[Ca^{2+}]_i$ in 0·5 mM $[Ca^{2+}]_o$ was subtracted from $[Ca^{2+}]_i$ in higher $[Ca^{2+}]_o$ and the data were normalized by setting the maximum increase in $[Ca^{2+}]_i$ to be 1·0. $[Ca^{2+}]_i$ steeply increased with an elevation of $[Ca^{2+}]_o$ from 0·5 to 2 mM and saturated at 3–4 mM $[Ca^{2+}]_o$. With higher $[Ca^{2+}]_o$, $[Ca^{2+}]_i$ tended to decrease. The apparent K_d was estimated to be about 1·8 mM. $[Ca^{2+}]_i$ in 3 mM-Ca^{2+} medium was $188{\cdot}9 \pm 40{\cdot}5\%$ ($n = 12$) of that in 0·5 mM-Ca^{2+} medium.

Effect of TTX on membrane potential and $[Ca^{2+}]_i$

The previous data suggest that increase in duration of the action potential in high $[Ca^{2+}]_o$ may be accompanied by an enhancement of voltage-gated Ca^{2+} current which causes the rise in $[Ca^{2+}]_i$. To clarify the involvement of Ca^{2+} action potentials in the increase in $[Ca^{2+}]_i$, the membrane potential was recorded in medium containing 10 μM-TTX. As shown in Fig. 7*B*, the increase of $[Ca^{2+}]_o$ from 0·5 to 3 mM evoked repetitive action potentials associated with a membrane depolarization and $[Ca^{2+}]_i$ was also increased. These observations further support the hypothesis that Ca^{2+} action potentials are involved in the rise of $[Ca^{2+}]_i$ evoked by high $[Ca^{2+}]_o$.

Membrane conductance increase and a rise in $[Ca^{2+}]_i$ in high $[Ca^{2+}]_o$ under voltage clamp

In order to examine the underlying ionic mechanisms in the membrane depolarization caused by high $[Ca^{2+}]_o$ and to examine whether Ca^{2+} influx through

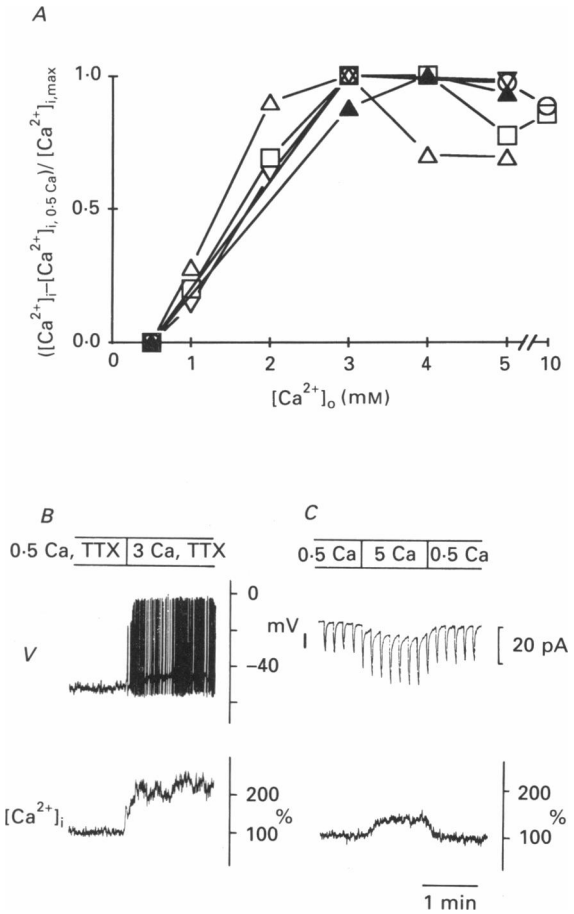

Fig. 7. *A*, the relationship between the increase in $[Ca^{2+}]_i$ and $[Ca^{2+}]_o$. The ordinate indicates the amplitude of integrated $[Ca^{2+}]_i$ normalized by setting the basal level to be 0 and the maximum increase in amplitude to be 1·0. The abscissa indicates $[Ca^{2+}]_o$. Each symbol represents data obtained from a single cell. *B*, changes of membrane potential (upper panel) and $[Ca^{2+}]_i$ (lower panel) in 3 mM-Ca^{2+} medium containing 10 μM-TTX, recorded under current clamp with the perforated whole-cell-clamp technique. The patch electrode contained the standard internal solution. *C*, changes of membrane current (upper panel) and $[Ca^{2+}]_i$ (lower panel) in 5 mM $[Ca^{2+}]_o$, recorded under voltage clamp with the perforated whole-cell-clamp technique. The holding potential was −67 mV and 1000 ms hyperpolarizing pulse of 30 mV amplitude was applied every 10 s. The patch electrode contained the standard internal solution.

voltage-gated channels is the sole mechanism in increasing $[Ca^{2+}]_i$, the membrane conductance and $[Ca^{2+}]_i$ were measured under voltage clamp. Figure 7*C* shows representative records of the membrane current (upper panel) and $[Ca^{2+}]_i$ (lower panel) in high $[Ca^{2+}]_o$, in which the membrane potential was clamped at −67 mV and 1 s hyperpolarizing voltage pulses of 30 mV amplitude were applied every 10 s. When $[Ca^{2+}]_o$ was increased from 0·5 to 5 mM, the current amplitude at the holding

potential increased due to an increase in membrane conductance. In addition, $[Ca^{2+}]_i$ steadily increased in high $[Ca^{2+}]_o$. Because the membrane potential was held at -67 mV which was below the threshold for voltage-gated Ca^{2+} channels, the increase in $[Ca^{2+}]_i$ was ascribed to a mechanism other than Ca^{2+} influx through such channels. To further rule out the involvement of voltage-gated Ca^{2+} channels, the membrane potential was held at -87 mV and high $[Ca^{2+}]_o$ was applied. An increase in $[Ca^{2+}]_i$ was also observed under this holding potential. During application of high $[Ca^{2+}]_o$, depolarizing pulses to -67 mV did not increase $[Ca^{2+}]_i$ (data not shown). If Ca^{2+} influx through voltage-gated channels was involved in the increase in $[Ca^{2+}]_i$ under the holding potential of -67 mV (Fig. 7*C*), $[Ca^{2+}]_i$ should increase by membrane depolarization from -87 to -67 mV. In addition, when the membrane was depolarized from -67 mV in 5 mM-Ca^{2+} medium, an increase in $[Ca^{2+}]_i$ was observed at potential steps to greater than -37 mV (data not shown), a finding further confirming that voltage-gated Ca^{2+} channels are not involved in the steady increase in $[Ca^{2+}]_i$.

Membrane currents measured in 0·5 and 5 mM-Ca^{2+} media are shown in panels *A* and *B*, respectively, of Fig. 8. The amplitude of the current at the end of the pulse is plotted against the membrane potential in Fig. 8*C*. The current in 0·5 mM-Ca^{2+} was subtracted from that in 5 mM-Ca^{2+} to obtain the high $[Ca^{2+}]_o$-induced current (Fig. 8*D*). The *I–V* relation of high $[Ca^{2+}]_o$-induced current in Fig. 8*D* is plotted against the membrane potential in Fig. 8*E* (○), where the data from two other cells are included (●, △). Extrapolating from these *I–V* relations, the reversal potential of high $[Ca^{2+}]_o$-induced current was -20 to 0 mV, suggesting an involvement of Na^+, Ca^{2+} or Cl^-, or a combination of many ions.

The upper panel in Fig. 9*A* shows the change of the membrane current obtained in Na^+-free medium. The membrane potential was held at -67 mV. Under this condition, an increase of $[Ca^{2+}]_o$ from 0·5 to 5 mM caused little apparent increase in membrane conductance. A similar result was obtained in three other cells. These data indicate that the membrane depolarization caused by high $[Ca^{2+}]_o$ is due to an increased permeability to Na^+ ions. However, in Na^+-free medium $[Ca^{2+}]_i$ increased following elevation of $[Ca^{2+}]_o$ to 5 mM. In the lower panel of Fig. 9*A* it can be seen that this increase was composed of an initial transient increase and a subsequent sustained increase. An alteration of Na^+-containing medium to Na^+-free medium did not affect $[Ca^{2+}]_i$.

K^+ conductance increase associated with the transient increase in $[Ca^{2+}]_i$

The upper panel in Fig. 9*B* depicts a less frequently observed response of the membrane conductance change to high $[Ca^{2+}]_o$. Prior to a rise in the inward current, a transient increase in current in the opposite direction was observed at the holding potential of -67 mV. The hyperpolarizing potential step to -97 mV revealed that during this transient the membrane conductance was increased, indicating that this was an outward current (see arrow). The equilibrium potential of Cl^- ions is about -30 mV and those of Na^+ and Ca^{2+} are at more depolarized levels, suggesting that the transient outward current was caused by a permeability increase to K^+ ions. As shown in the lower panel, it may be seen that in this case the $[Ca^{2+}]_i$ increase in response to 5 mM-Ca^{2+} was composed of a transient increase and a subsequent

sustained increase (compare to Fig. 7*C*). The transient K^+ current was evoked during the transient increase in $[Ca^{2+}]_i$, suggesting that this K^+ current may be carried by a Ca^{2+}-activated K^+ channel. Membrane hyperpolarization *per se* did not cause an increase in $[Ca^{2+}]_i$ under voltage clamp (see below), suggesting that Ca^{2+}-activated

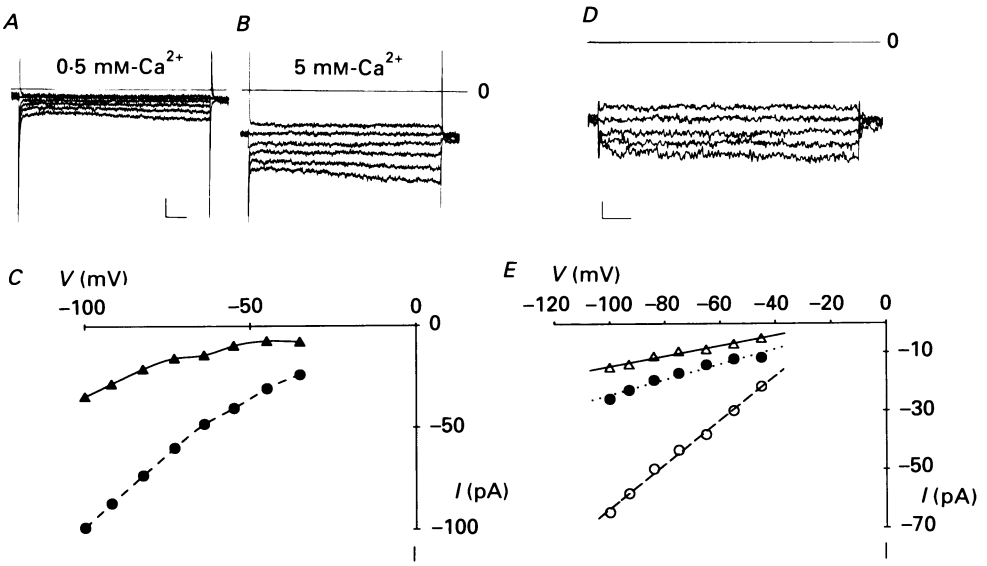

Fig. 8. High $[Ca^{2+}]_o$-induced current. *A* and *B*, membrane currents in 0·5 mM-Ca^{2+} and 5 mM-Ca^{2+} media recorded under voltage clamp with the perforated whole-cell-clamp technique. The patch electrode contained the standard internal solution. The holding potential was −67 mV. Membrane currents at every 10 mV potential step from −107 to −57 mV are shown. Leakage current was not subtracted. The continuous line indicates the zero current level. Current amplitude and time scale bar are equal to 20 pA and 50 ms, respectively. *C*, *I–V* relations of the records in *A* (▲) and *B* (●). Series resistance of the patch electrode was 40 MΩ. The clamped potential level was corrected by the formula shown in Methods. *D*, high $[Ca^{2+}]_o$-induced current which was obtained by subtracting the membrane current in *A* from that in *B*. Subtracted currents at −97, −87, −77, −67 and −57 mV are shown. The continuous line indicates the zero current level. Current amplitude and time scale bar are equal to 10 pA and 50 ms, respectively. *E*, *I–V* relations of high $[Ca^{2+}]_o$-induced current. ○, the data in *D*; ● and △, data obtained from two other cells. Lines were drawn by eye.

K^+ conductance is activated by the rise in $[Ca^{2+}]_i$ and the membrane hyperpolarizations observed under current clamp (Fig. 6*B*) may be caused by this transient K^+ current recorded under voltage clamp.

Mobilization of Ca^{2+} *from an intracellular store in the generation of the transient rise in* $[Ca^{2+}]_i$

To examine whether the rise in $[Ca^{2+}]_i$ under voltage clamp was caused by an influx through voltage-independent channels or by a mobilization from internal Ca^{2+} stores, 5 mM $[Ca^{2+}]_o$ was briefly (500 ms) applied by the puff method (Fig. 9*C*). With

this brief application of high $[Ca^{2+}]_o$, $[Ca^{2+}]_i$ transiently increased and reached its maximum 10–15 s after termination of high $[Ca^{2+}]_o$ application. Corresponding to the transient increase in $[Ca^{2+}]_i$, a small outward current was evoked. Because the 0·5 mM-Ca^{2+} medium was continuously perfused and because the glass capillary

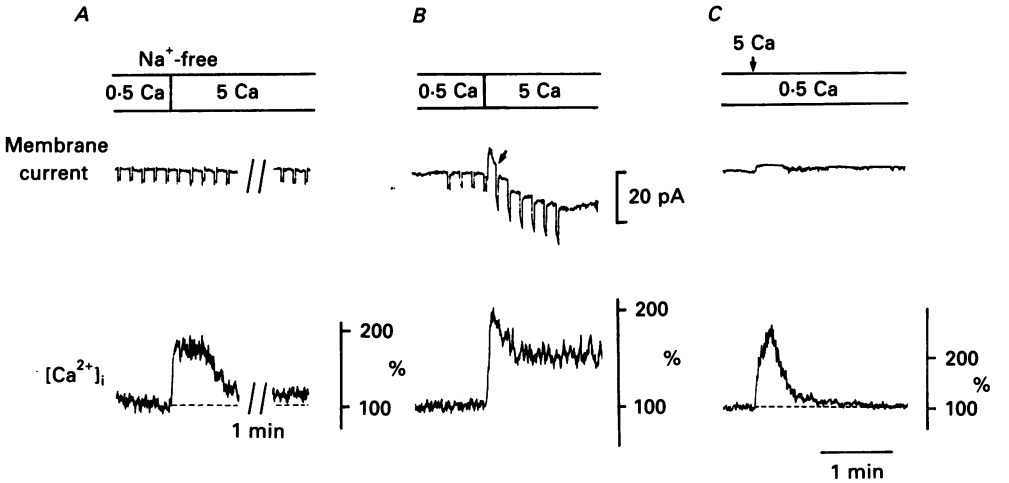

Fig. 9. *A*, changes of membrane current (upper panel) and $[Ca^{2+}]_i$ (lower panel) in 5 mM-$[Ca^{2+}]_o$ recorded in Na^+-free medium under voltage clamp with the perforated whole-cell-clamp technique. The holding potential was −67 mV. Hyperpolarizing pulse (1000 ms) of 30 mV amplitude was applied every 10 s. The dashed line in $[Ca^{2+}]_i$ indicates the basal level of $[Ca^{2+}]_i$ in 0·5 mM-Ca^{2+}, Na^+-free medium. *B*, changes of membrane current (upper panel) and $[Ca^{2+}]_i$ (lower panel) in high $[Ca^{2+}]_o$. Holding potential was −67 mV. A hyperpolarizing pulse of 1000 ms duration and 30 mV amplitude was applied every 10 s. The arrow indicates the membrane conductance increase during a transient outward current. *C*, changes of membrane current (upper panel) and $[Ca^{2+}]_i$ (lower panel) with brief (500 ms) application of 5 mM $[Ca^{2+}]_o$ by the puff method. The 0·5 mM-Ca^{2+} medium was continuously perfused during recordings and the timing of 5 mM $[Ca^{2+}]_o$ application is indicated by an arrow. The patch electrode contained the standard internal solution in *A*, *B* and *C*.

containing the 5 mM-Ca^{2+} medium was withdrawn immediately after application, the cell should not have been exposed to 5 mM $[Ca^{2+}]_o$ for more than 500 ms. If the transient rise in $[Ca^{2+}]_i$ was entirely composed of the Ca^{2+} influx, it should not continue to increase after the termination of high $[Ca^{2+}]_o$ application. Therefore it was concluded that the mobilization of Ca^{2+} from an intracellular store is involved in the generation of the initial transient rise in $[Ca^{2+}]_i$. After the transient increase, $[Ca^{2+}]_i$ returned close to the basal level and a sustained increase was not clearly observed, suggesting that the presence of high $[Ca^{2+}]_o$ was required for the maintenance of the sustained increase.

In agonist-stimulated mast cells and human leukaemic T cells it has been reported that hyperpolarization increases $[Ca^{2+}]_i$ (Penner, Matthews & Neher, 1988; Lewis & Cahalan, 1989). In rMTC 44-2 cells the membrane hyperpolarization did not increase $[Ca^{2+}]_i$ in high $[Ca^{2+}]_o$ (Figs 7*C* and 9*A* and *B*). Similarly further hyperpolarization (up to −130 mV) or for longer duration (up to 30 s) did not increase $[Ca^{2+}]_i$.

Therefore the increase in $[Ca^{2+}]_i$ in rMTC 44-2 cells is not likely to be due to the voltage-independent Ca^{2+} channel described in these cells.

Dependence of $[Ca^{2+}]_i$ *on* $[Ca^{2+}]_o$ *under voltage clamp*

The increase in $[Ca^{2+}]_i$ in response to elevation of $[Ca^{2+}]_o$ shown in Fig 9*A* and *B* was composed of an initial transient increase and a subsequent sustained increase.

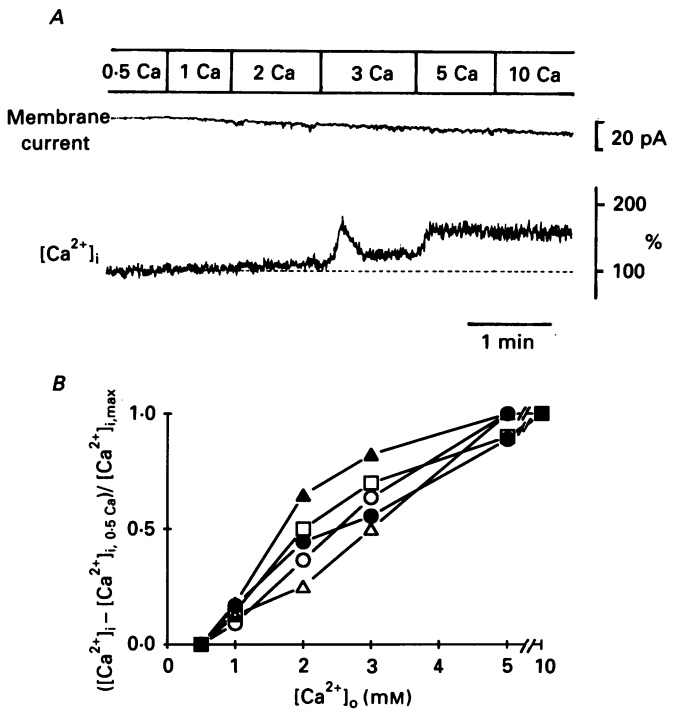

Fig. 10. *A*, changes of membrane current (upper panel) and $[Ca^{2+}]_i$ (lower panel) during successive increases of $[Ca^{2+}]_o$ from 0·5 to 10 mM, recorded under voltage clamp with the perforated whole-cell-clamp technique. The holding potential was −67 mV. The dashed line in $[Ca^{2+}]_i$ indicates the basal level of $[Ca^{2+}]_i$ in 0·5 mM-Ca^{2+} medium. The patch electrode contained the standard internal solution. *B*, the relationship between the amplitude of sustained increase and $[Ca^{2+}]_o$. The ordinate indicates the amplitude of sustained increase in $[Ca^{2+}]_i$ normalized by setting the basal level to the 0 and the amplitude of maximum increase to be 1·0. The abscissa indicates $[Ca^{2+}]_o$. Each symbol represents data obtained from a single cell.

However, the initial transient increase was not always observed (see Fig. 7*C*). Figure 10*A* shows the changes of membrane current and $[Ca^{2+}]_i$ during a progressive increase of $[Ca^{2+}]_o$ from 0·5 to 10 mM. An initial transient increase in $[Ca^{2+}]_i$ was observed only in 3 mM-Ca^{2+} medium. Including other experiments, the initial transient increase was observed in none of twenty cells in 1 mM-Ca^{2+} medium, in two out of twenty-six cells in 2 mM-Ca^{2+} medium, in six out of twenty-three cells in 3 mM-Ca^{2+} medium and in twelve out of fifty-eight cells in 5 mM-Ca^{2+} medium. These data

suggest that the appearance of the initial transient increase was dependent on $[Ca^{2+}]_o$. However, the peak amplitude of the initial transient increase in $[Ca^{2+}]_i$ did not seem to depend on $[Ca^{2+}]_o$ and it was $202{\cdot}8 \pm 63{\cdot}2\%$ of $[Ca^{2+}]_i$ in 0·5 mM-Ca^{2+} medium.

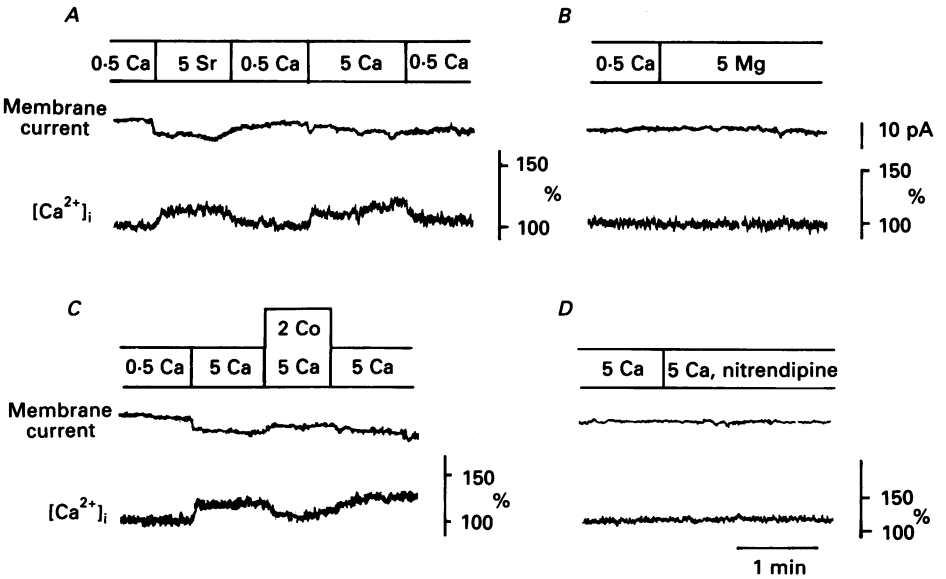

Fig. 11. Effect of other divalent cations and dihydropyridines on the membrane current (upper panel) and $[Ca^{2+}]_i$ (lower panel), recorded under voltage clamp with the perforated whole-cell-clamp technique. The holding potential was −65 to −67 mV. The patch electrode contained the standard internal solution. 5 mM-Sr^{2+} medium (*A*) and 5 mM-Mg^{2+} medium (*B*) did not contain Ca^{2+} ions. Nitrendipine in *D* indicates the application of 1 μM-nitrendipine which was added to 5 mM-Ca^{2+} medium.

In contrast to the initial transient increase, there was a consistent relationship between $[Ca^{2+}]_o$ and the sustained increase of $[Ca^{2+}]_i$ (62/69, with 3 or 5 mM $[Ca^{2+}]_o$). As shown in Fig. 10*A*, the amplitude of the sustained increase of $[Ca^{2+}]_i$ was dependent on $[Ca^{2+}]_o$ and was close to saturation with 5 mM $[Ca^{2+}]_o$. Dose dependence in five representative cells is shown in Fig. 10*B*. The apparent K_d was estimated to be about 2·5 mM. The amplitude of sustained phase of $[Ca^{2+}]_i$ in 5 mM $[Ca^{2+}]_o$ was $120{\cdot}9 \pm 18{\cdot}9\%$ (103–194%, $n = 58$) of the basal level, this value being about $\frac{1}{4}$ of the increment of $[Ca^{2+}]_i$ in 3 mM-Ca^{2+} medium observed under current clamp (see above).

Effect of other divalent cations and dihydropyridines

To examine whether the effects of external Ca^{2+} on the membrane current and $[Ca^{2+}]_i$ are specific to Ca^{2+} ions, the effects of other divalent cations on the membrane current and $[Ca^{2+}]_i$ were examined. As shown in Fig. 11*A*, 5 mM-Sr^{2+} increased the membrane current at −67 mV as well as increased $[Ca^{2+}]_i$, whereas 5 mM-Mg^{2+} (Fig. 11*B*) and 5 mM Co^{2+} (not shown) had little effect. Addition of 2 mM-Co^{2+} to 5 mM-Ca^{2+} medium inhibited both increases of the membrane current and $[Ca^{2+}]_i$

(Fig. 11*C*). The abilities of these divalent cations to modulate membrane current and alter $[Ca^{2+}]_i$ are similar to those on the voltage-gated Ca^{2+} channel (Hagiwara & Byerley, 1981). Addition of 1 μM-nitrendipine either to 5 mM-Ca^{2+} (Fig. 11*D*) or to 0·5 mM-Ca^{2+} medium (not shown) had no effect. Similarly, addition of 1 μM-Bay

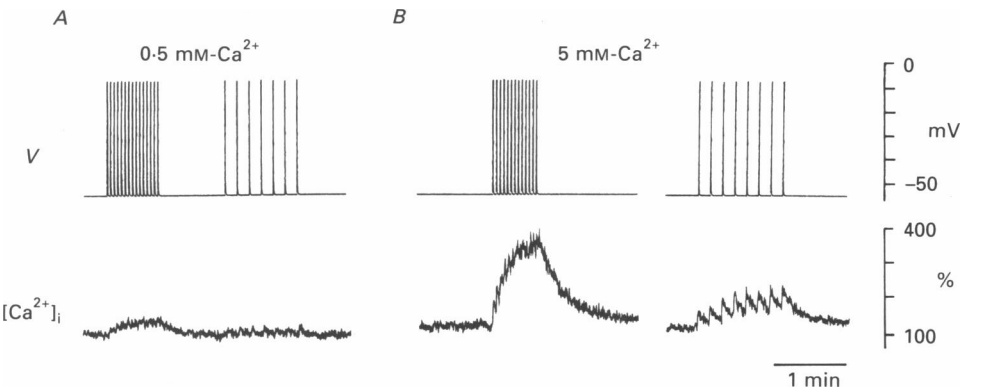

Fig. 12. Changes of $[Ca^{2+}]_i$ by depolarizing pulses with different intervals, recorded under voltage clamp with the perforated whole-cell-clamp technique. Records in *A* were obtained in 0·5 mM-Ca^{2+} medium and those in *B* in 5 mM-Ca^{2+} medium. Upper panel indicates the pattern for applying 400 ms depolarizing pulses and lower panel, $[Ca^{2+}]_i$. The holding potential was −55 mV. A depolarizing pulse to −5 mV was applied at every 3 or 10 s. The patch electrode contained the standard internal solution.

K8644 to 0·5 or 5 mM-Ca^{2+} medium had no effect (not shown). This suggests that a dihydropyridine-like receptor does not mediate these effects on membrane current and $[Ca^{2+}]_i$ in rMTC 44-2 cells.

Relationship between the frequency of depolarizing pulses and $[Ca^{2+}]_i$ *increase under voltage clamp*

Under current clamp, the action potential frequency often decreased in high $[Ca^{2+}]_o$ and a transient rise in $[Ca^{2+}]_i$ was observed corresponding to a single action potential with a prolonged duration (Fig. 5*B*, 3 mM $[Ca^{2+}]_o$; Fig. 6*B*, 5 mM $[Ca^{2+}]_o$). In order to examine why the occurrence of a transient rise in $[Ca^{2+}]_i$ is restricted to high $[Ca^{2+}]_o$ and why $[Ca^{2+}]_i$ remains elevated in spite of the reduction of action potential frequency in high $[Ca^{2+}]_o$, the following experiments were performed under voltage clamp. Figure 12 shows the changes in $[Ca^{2+}]_i$ (lower panels) under voltage clamp in 0·5 (*A*) and 5 mM-Ca^{2+} (*B*) media in which 50 mV pulses of 400 ms duration were given from the holding potential of −55 mV according to the pulse patterns shown in the upper panels. When the depolarizing pulse was applied every 3 s (pulse pattern on the left of the upper panels), the increase in $[Ca^{2+}]_i$ in 5 mM $[Ca^{2+}]_o$ was much greater than that in 0·5 mM $[Ca^{2+}]_o$. When the depolarizing pulse was applied every 10 s (pulse pattern on the right of the upper panels), the rise in $[Ca^{2+}]_i$ was too small to be clearly seen in 0·5 mM $[Ca^{2+}]_o$, whereas in 5 mM $[Ca^{2+}]_o$ $[Ca^{2+}]_i$ transiently increased with each pulse and the baseline of $[Ca^{2+}]_i$ was also elevated. The elevated baseline of $[Ca^{2+}]_i$ returned close to the original level when the pulse interval was

longer than 20 s (not shown). These results could be applied to the relationship between the action potential frequency and the changes in $[Ca^{2+}]_i$ recorded under current clamp. When the action potential frequency was high, the increase in $[Ca^{2+}]_i$ seemed to be composed of the summation of increases in $[Ca^{2+}]_i$. When the action

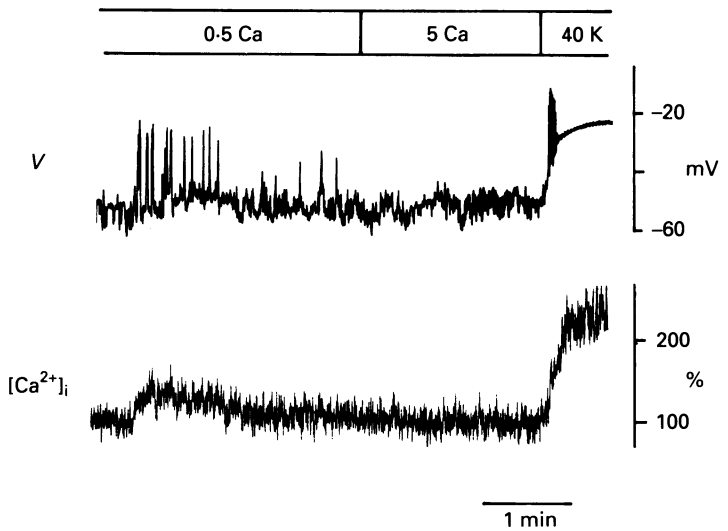

Fig. 13. Changes of membrane potential (upper panel) and $[Ca^{2+}]_i$ (lower panel) in a GH_3 cell. The methods for measurement and solutions are the same as used in rMTC cells. 40 K means the medium containing 40 mM-K^+ and 1 mM-Ca^{2+}.

potential frequency was low but the Ca^{2+} current was large, the transient rise in $[Ca^{2+}]_i$ could be observed and $[Ca^{2+}]_i$ did not greatly decrease during the pause of action potentials because the relaxation time of $[Ca^{2+}]_i$ was longer than the interval of action potential occurrence. Only when the action potential was inhibited for a longer period as compared with the relaxation time of $[Ca^{2+}]_i$ (for example, see DC in Fig. 5*B*) did $[Ca^{2+}]_i$ prominently decrease.

The effect of high $[Ca^{2+}]_o$ *on* GH_3 *cells*

It may be proposed that in other types of cells increasing $[Ca^{2+}]_o$ can raise $[Ca^{2+}]_i$ due to an enhanced Ca^{2+} influx and that the observed changes are not specific to rMTC 44-2 cells. However, in human osteosarcoma cells and rat fibroblasts, Fried & Tashjian (1986) have shown that increasing $[Ca^{2+}]_o$ from 1 to 4 mM has little effect on $[Ca^{2+}]_i$. To similarly rule out this proposal in excitable secretory cells, rat pituitary GH_3 cells were used, because these cells exhibit Na^+- and Ca^{2+}-dependent action potentials (Kidokoro, 1975; Biales, Dichter & Tischler, 1977) and because they are endocrine cells similar to rMTC 44-2 cells. Figure 13 shows the changes of the membrane potential and $[Ca^{2+}]_i$ in a GH_3 cell recorded with the same methods as used in rMTC 44-2 cells. In 0·5 mM-Ca^{2+} medium spontaneous action potentials were observed. An increase in $[Ca^{2+}]_i$ was seen during a burst of action potentials. The application of 5 mM $[Ca^{2+}]_o$ did not depolarize the membrane, nor did it increase

$[Ca^{2+}]_i$. The spontaneous action potentials were inhibited in 5 mM-Ca^{2+} medium. The change of 5 mM-Ca^{2+} medium to 40 mM-K^+, 1 mM-Ca^{2+} medium caused a prominent membrane depolarization accompanied by an increase in $[Ca^{2+}]_i$. Similar results were observed in GH_3 cells which did not show spontaneous action potentials in 0·5 mM-Ca^{2+} medium (data not shown). Therefore it was concluded that the observed changes in rMTC 44-2 cells were not due to non-specific effects of high $[Ca^{2+}]_o$.

DISCUSSION

The present study revealed that rMTC 44-2 cells possess several classes of ionic channels, including voltage-gated Na^+ channels, two types of voltage-gated Ca^{2+} channels, A-type K^+ channels, delayed K^+ channels and inward-rectifying K^+ channels. Elevation of $[Ca^{2+}]_o$ increased Na^+ conductance, which depolarized the membrane. $[Ca^{2+}]_i$ also increased in high $[Ca^{2+}]_o$. Under current clamp, the existence of action potentials was important for increasing $[Ca^{2+}]_i$ in high $[Ca^{2+}]_o$ although action potential frequency was not correlated to a rise in $[Ca^{2+}]_i$. Voltage-clamp experiments revealed the existence of additional mechanisms in increase of $[Ca^{2+}]_i$ in high $[Ca^{2+}]_o$ which were different from Ca^{2+} influx through voltage-gated channels.

Voltage-gated channels in rMTC 44-2 cells

Na^+ and Ca^{2+} action potentials in rMTC 44-2 cells have already been reported by Sand *et al.* (1981). Human MTC cells are also capable of generating Na^+ and Ca^{2+} action potentials (Sand, Jonsson, Nilsen, Holm & Gautvik, 1986) and recently Kawa (1988) has reported voltage-gated Na^+, Ca^{2+} and K^+ channels in chick calcitonin-secreting cells. Because calcitonin-secreting cells are thought to be of neural crest origin (Ozawa & Sand, 1986), these voltage-gated channels may be present in calcitonin-secreting cells of other species. In human MTC cells Sand *et al.* (1986) have reported that lowering $[Ca^{2+}]_o$ hyperpolarizes the membrane concomitant with a conductance decrease. This result is consistent with the present result. However, they have reported that the reversal potential of the response is -66 mV, and that the reduced conductance is that of K^+ or Cl^- ions (or both). In rMTC cells the ions involved were Na^+. In human MTC cells the reversal potential appears to be more depolarized than the equilibrium potential of K^+ ions, so that Na^+ conductance may also be increased. However, at present there is no other explanation for this discrepancy.

Membrane conductance increase in high $[Ca^{2+}]_o$

The membrane depolarization in high $[Ca^{2+}]_o$ was caused by the permeability increase to Na^+ ions. The reversal potential was estimated to be -20 to 0 mV (Fig. 8*E*), suggesting that this Na^+ current was carried through non-selective cation channels. Under voltage clamp $[Ca^{2+}]_i$ increased during the Na^+ permeability increase. Therefore this Na^+ conductance might be due to Ca^{2+}-activated non-selective cation channels (Colquhoun, Neher, Reuter & Stevens, 1981; Yellen, 1982). Na^+ conductance increase was observed in some cells which did not show a detectable rise in $[Ca^{2+}]_i$ (not shown), a finding in favour of the notion that Na^+ conductance was

directly or indirectly increased by $[Ca^{2+}]_o$ and was independent of $[Ca^{2+}]_i$. However, it is still possible that the Na^+ conductance was activated by a small increase in $[Ca^{2+}]_i$ which could not be detected by Fura-2.

The reduction of action potential frequency in high $[Ca^{2+}]_o$ and a transient increase in $[Ca^{2+}]_i$ corresponding to a single action potential under current clamp

In high $[Ca^{2+}]_o$ the frequency of action potentials did not always increase but often decreased. Although one reason for the decrease of the action potential frequency in higher $[Ca^{2+}]_o$ may be the surface potential effect of Ca^{2+} ions, the action potential frequency prominently decreased in Figs 5*B* (3 mM $[Ca^{2+}]_o$) and 6*B* (5 mM $[Ca^{2+}]_o$), where the action potential was followed by a prolonged after-hyperpolarization probably due to Ca^{2+}-activated K^+ conductance increase. Therefore it seemed that the reduction of action potential frequency in high $[Ca^{2+}]_o$ was due to the prolonged after-hyperpolarization. The amplitude of Ca^{2+}-activated K^+ current and its sensitivity to $[Ca^{2+}]_i$ may vary among cells, which could explain the variability in action potential frequency among cells in high $[Ca^{2+}]_o$.

Under current clamp a transient increase in $[Ca^{2+}]_i$ was observed corresponding to a single action potential with a prolonged duration in high $[Ca^{2+}]_o$ only when the action potential frequency decreased. In other cases such a transient increase in $[Ca^{2+}]_i$ was not observed. It has been reported that large fluctuations of $[Ca^{2+}]_i$ are correlated with spontaneous action potentials in GH_3 cells (Schlegel, Winiger, Mollard, Vacher, Waurin, Zahnd, Wollheim & Dufy, 1987). In their experiment the extracellular Ca^{2+} concentration was 10 mM, so that their result appears to be compatible with the action potential with a prolonged duration in higher $[Ca^{2+}]_o$ in the present study.

Dependence of $[Ca^{2+}]_i$ on $[Ca^{2+}]_o$

Under current clamp, $[Ca^{2+}]_i$ steeply increased with an elevation of $[Ca^{2+}]_o$ from 0·5 to 2 mM and saturated at 3–4 mM $[Ca^{2+}]_o$. Hormone secretion of rMTC 44-2 cells is also stimulated by $[Ca^{2+}]_o$ within this range and saturates at about 4 mM $[Ca^{2+}]_o$ (Zeytinoglu *et al.* 1983), indicating the close relationship between hormone secretion and $[Ca^{2+}]_i$. With $[Ca^{2+}]_o$ higher than 3 or 4 mM, $[Ca^{2+}]_i$ tended to decrease, which may be caused by a further reduction of action potential frequency in higher $[Ca^{2+}]_o$. The plateau phase of $[Ca^{2+}]_i$ under voltage clamp was also dependent on $[Ca^{2+}]_o$ but it saturated with $[Ca^{2+}]_o$ higher than 5 mM. Although the saturated amplitude of plateau phase was about $\frac{1}{4}$ of that of $[Ca^{2+}]_i$ under current clamp, the plateau phase may be involved in hormone secretion in higher $[Ca^{2+}]_o$, where Ca^{2+} influx through voltage-gated channels decreases due to the reduction of action potential frequency.

Three components in the increase in $[Ca^{2+}]_i$

The present results indicated that there were three components in the increase in $[Ca^{2+}]_i$; an influx through voltage-gated Ca^{2+} channels, an initial transient increase under voltage clamp and a sustained increase under voltage clamp. The influx through voltage-gated Ca^{2+} channels accounted for the increase in $[Ca^{2+}]_i$ under current clamp and the membrane depolarization due to the increased Na^+ permeability took a part in evoking action potentials. The initial transient increase

under voltage clamp was ascribed to the mobilization of Ca^{2+} ions from the internal store. Although the mechanism for the sustained increase under voltage clamp was not clarified compared with the other two mechanisms, the presence of high $[Ca^{2+}]_o$ was required and external Co^{2+} blocked it. These findings might be ascribed to some ion exchange mechanisms or to the influx through voltage-independent Ca^{2+} channels although Ca^{2+} current through such channels could not be detected (Fig. 9*A*). Voltage-independent Ca^{2+} channels reported in mast cells (Penner *et al.* 1988) and in human leukaemic T cells (Lewis & Cahalan, 1989) could not account for the sustained increase in rMTC cells because membrane hyperpolarization did not increase $[Ca^{2+}]_i$.

In rat GH_3 cells thyrotrophin-releasing hormone (TRH) evokes a transient rise in $[Ca^{2+}]_i$ that is followed by a sustained rise when the membrane potential is held at the holding potential of -60 to -70 mV (Benham, 1989). Membrane hyperpolarization does not increase $[Ca^{2+}]_i$ in GH_3 cells. The transient increase evoked by TRH in GH_3 cells was independent of $[Ca^{2+}]_o$, whereas the sustained increase was dependent on $[Ca^{2+}]_o$. Thus, the changes of $[Ca^{2+}]_i$ in GH_3 cells caused by TRH under voltage clamp are similar to those observed in high $[Ca^{2+}]_o$ in rMTC 44-2 cells, although the mechanism causing the membrane depolarization is ascribed to the K^+ conductance decrease in GH_3 cells (Ozawa, 1981). The effects of divalent cations on membrane current and $[Ca^{2+}]_i$ in rMTC 44-2 cells were similar to those on voltage-gated Ca^{2+} channels (Hagiwara & Byerley, 1981), in which the existence of high-affinity Ca^{2+} binding sites is implicated (Kostyuk, Mironov & Schuba, 1983; Almers, McCleskey & Palade, 1984; Hess & Tsien, 1984). In GH_3 cells high $[Ca^{2+}]_o$ did not increase $[Ca^{2+}]_i$. Therefore it seems likely that rMTC 44-2 cells possess specific Ca^{2+} binding sites or receptors on the cell surface which sense external Ca^{2+} concentrations. The mechanisms transmitting these signals into cytoplasm might be in part analogous to TRH receptors.

We thank Dr A. H. Tashjian, Jr for providing rMTC 44-2 cell line, and Drs Y. Kidokoro, Y. Harada, G. T. Eddlestone, B. Ribalet and S. Krasne for valuable comments and suggestions. We also thank Dr J. Schroeder for his help in measuring $[Ca^{2+}]_i$. This work was supported by USPHS grant NS09012 and by a grant from the Muscular Dystrophy Association.

REFERENCES

ALMERS, W., MCCLESKEY, E. W. & PALADE, P. T. (1984). A non-selective cation conductance in frog muscle membrane blocked by micromolar external calcium ions. *Journal of Physiology* **353**, 565–584.

BENHAM, C. D. (1989). Voltage-gated and agonist-mediated rises in intracellular Ca^{2+} in rat clonal pituitary cells (GH_3) held under voltage clamp. *Journal of Physiology* **415**, 143–158.

BIALES, B., DICHTER, M. A. & TISCHLER, A. (1977). Sodium and calcium action potentials in pituitary cells. *Nature* **267**, 172–174.

BRUCE, B. R. & ANDERSON, N. C. JR (1979). Hyperpolarization in mouse parathyroid cells by low calcium. *American Journal of Physiology* **236**, C15–21.

COLQUHOUN, D., NEHER, E., REUTER, H. & STEVENS, C. F. (1981). Inward current channels activated by intracellular Ca in cultured cardiac cells. *Nature* **294**, 752–754.

COOPER, C. W., BOROSKY, S. A., FARRELL, P. E. & STEINSLAND, O. S. (1986). Effects of the calcium channel activator Bay-K-8644 on *in vitro* secretion of calcitonin and parathyroid hormone. *Endocrinology* **118**, 545–549.

FRIED, R. M. & TASHJIAN, A. H. JR (1986). Unusual sensitivity of cytosolic free Ca^{2+} to changes in extracellular Ca^{2+} in rat C-cells. *Journal of Biological Chemistry* **261**, 7699–7674.

GAGEL, R. F., ZEYTINOGLU, F. N., VOELKEL, E. F. & TASHJIAN, A. H. JR (1980). Establishment of a calcitonin-producing rat medullary thyroid carcinoma cell line. II. Secretory studies of the tumor and cells in culture. *Endocrinology* **107**, 516–523.

HAGIWARA, S. (1983). K Channels. In *Membrane Potential-Dependent Ion Channels in Cell Membrane*, pp. 61–86. Raven Press, New York.

HAGIWARA, S. & BYERLEY, L. (1981). Calcium channel. *Annual Review of Neuroscience* **4**, 69–125.

HALLER-BREM, S., MUFF, R., PETERMANN, J. B., BORN, W., ROOS, B. A. & FISCHER, J. A. (1987). Role of cytosolic free calcium concentration in the secretion of calcitonin gene-related peptide and calcitonin from medullary thyroid carcinoma cells. *Endocrinology* **121**, 1272–1277.

HAMILL, O. P., MARTY, A., NEHER, E., SAKMANN, B. & SIGWORTH, F. J. (1981). Improved patch-clamp techniques for high-resolution current recording from cells and cell-free membrane patches. *Pflügers Archiv* **391**, 85–100.

HESS, P. & TSIEN, R. W. (1984). Mechanism of ion permeation through calcium channels. *Nature* **309**, 453–456.

HISHIKAWA, R., FUKASE, M., TAKENAKA, M. & FUJITA, T. (1985). Effect of calcium channel agonist Bay K 8644 on calcitonin secretion from a rat c-cell line. *Biochemical and Biophysical Research Communications* **130**, 454–459.

HORN, R. & MARTY, A. (1988). Muscarinic activation of ionic currents measured by a new whole-cell recording method. *Journal of General Physiology* **92**, 145–159.

JACOB, R., MURPHY, E. & LIEBERMAN, M. (1987). Free calcium in isolated chick embryo heart cells measured using quin2 and fura-2. *American Journal of Physiology* **253**, C337–342.

KAWA, K. (1988). Voltage-gated sodium and potassium currents and their variation in calcitonin-secreting cells of the chick. *Journal of Physiology* **399**, 93–113.

KIDOKORO, Y. (1975). Spontaneous Ca action potentials in a clonal pituitary cell line and their relation to prolactin secretion. *Nature* **258**, 741–742.

KOSTYUK, P. G., MIRONOV, S. L. & SCHUBA, M. Y. (1983). Two ion-selecting filters in the calcium channel of the somatic membrane of mollusc. *Journal of Membrane Biology* **76**, 83–93.

KURTZ, A. & PENNER, R. (1989). Angiotensin II induces oscillations of intracellular calcium and blocks anomalous inward rectifying potassium current in mouse renal juxtaglomerular cells. *Proceedings of the National Academy of Sciences of the USA* **86**, 3423–3427.

LEWIS, R. S. & CAHALAN, M. D. (1989). Mitogen-induced oscillation of cytosolic Ca^{2+} and transmembrane Ca^{2+} current in human leukemic T cells. *Cell Regulation* **1**, 99–112.

LEWIS, D. L., GOODMAN, M. B., JOHN, P. A. & BARKER, J. L. (1988). Calcium currents and fura-2 signals in fluorescence-activated cell sorted lactotrophs and somatotrophs of rat anterior pituitary. *Endocrinology* **123**, 611–621.

LOPEZ-BARNEO, J. & ARMSTRONG, C. M. (1983). Depolarizing response of rat parathyroid cells to divalent cations. *Journal of General Physiology* **82**, 269–294.

MORRISSEY, J. J. & KLAHR, S. (1983). Dissociation of membrane potential and hormone secretion in bovine parathyroid cells. *American Journal of Physiology* **245**, E102–105.

MUFF, R., NEMETH, E. F., HALLER-BREM, S. & FISCHER, J. A. (1988). Regulation of hormone secretion and cytosolic Ca^{2+} by extracellular Ca^{2+} in parathyroid cells and c-cells: role of voltage-sensitive Ca^{2+} channels. *Archives of Biochemistry and Biophysics* **265**, 128–135.

NEMETH, E. F. & SCARPA, A. (1987). Rapid mobilization of cellular Ca^{2+} in bovine parathyroid cells evoked by extracellular divalent cations. Evidence for a cell surface calcium receptor. *Journal of Biological Chemistry* **262**, 5188–5196.

OZAWA, S. (1981). Biphasic effect of thyrotropin-releasing hormone on membrane K^+ permeability in rat clonal pituitary cells. *Brain Research* **209**, 240–244.

OZAWA, S. & SAND, O. (1986). Electrophysiology of excitable endocrine cells. *Physiological Review* **66**, 887–952.

PENNER, R., MATTHEWS, G. & NEHER, E. (1988). Regulation of calcium influx by second messengers in rat mast cells. *Nature* **334**, 499–504.

SAND, O., JONSSON, L., NILSEN, M., HOLM, R. & GAUTVIK, K. M. (1986). Electrophysiological properties of calcitonin-secreting cells derived from human medullary thyroid carcinoma. *Acta physiologica scandinavica* **126**, 173–179.

SAND, O., OZAWA, S. & GAUTVIK, K. M. (1981). Sodium and calcium action potentials in cells derived from a rat medullary thyroid carcinoma. *Acta physiologica scandinavica* **112**, 287–291.

SAND, O., OZAWA, S. & HOVE, K. (1981). Electrophysiology of cultured parathyroid cells from the goat. *Acta physiologica scandinavica* **113**, 45–50.

SCHLEGEL, W., WINIGER, B. P., MOLLARD, P, VACHER, P., WAURIN, F., ZAHND, G., WOLLHEIM, C. B. & DUFY, B. (1987). Oscillation of cytosolic Ca^{2+} in pituitary cells due to action potential. *Nature* **329**, 719–721.

SCHOBACK, D. M., MAMBRENO, L. A. & MCGHEE, J. G. (1988). High calcium and other divalent cations increase inositol triphosphate in bovine parathyroid cells. *Endocrinology* **123**, 382–389.

YAMASHITA, N. & HAGIWARA, S. (1990). High $[Ca^{2+}]_o$ causes membrane depolarization and $[Ca^{2+}]_i$ increase in a calcitonin-secreting rat cell line. *Biophysical Journal* **57**, 312*a*.

YELLEN, G. (1982). Single Ca^{2+}-activated nonselective cation channels in neuroblastoma. *Nature* **296**, 357–359.

ZEYTINOGLU, F., GAGEL, R. F., TASHJIAN, A. H. JR, HAMMER, R. A. & LEEMAN, S. E. (1983). Regulation of neurotensin release by a continuous line of mammalian C-cells: the role of biogenic amines. *Endocrinology* **112**, 1240–1246.